Süleyman Demirel Üniversitesi
Fen Bilimleri Enstitüsü Dergisi
Cilt 28, Sayı 3, 460-471, 2024

Süleyman Demirel University
Journal of Natural and Applied Sciences
Volume 28, Issue 3, 460-471, 2024

DOI: 10.19113/sdufenbed.1517015

Triflorometil içeren Yeni Azo-İmin Bileşikleri: Sentezi, Karakterizasyonu, *in siliko* ve *in vitro* Yöntemlerle Antioksidan Özelliklerinin Araştırılması

Tolga Acar YEŞİL[1*]

[1]Sinop Üniversitesi, Türkeli Meslek Yüksekokulu Mülkiyet Koruma ve Güvenlik Bölümü, 57900, Sinop, Türkiye

(Alınış / Received: 16.07.2024, Kabul / Accepted: 08.10.2024, Online Yayınlanma / Published Online: 23.12.2024)

Anahtar Kelimeler
Schiff Bazı,
CUPRAC Metod,
Antioksidan,
Moleküler Kenetlenme,
ADMEt

Öz: Bu çalışmada iki yeni molekül 4-((4-metoksifenil)diazenil)-2-(((4-(triflorometil)fenil)imino)metil)fenol (**3a**) ve 2-(((4-metoksifenil)imino) metil)-4-((4-(triflorometil)fenil)diazenil)fenol (**3b**) sentezlendi. **3a** ve **3b**'nin yapılarını doğrulamak için ^{1}H-NMR, FTIR, UV-vis ve Kütle analiz teknikleri kullanıldı. Sentezlenen bileşiklerin antioksidan özelliklerini araştırmak için CUPRAC *in vitro* antioksidan aktivite yöntemi de kullanıldı. Bileşiklerin ADME ve toksisite parametreleri de sırasıyla SwissADME, Protox-II web sunucuları kullanılarak hesaplandı. Sentezlenen bileşikler **3a** ve **3b**'nin potansiyel antioksidan özelliklerini araştırmak için PDB ID: Lipoksijenaz için 1N8Q, CYP2C9 için 1OG5, NADPH oksidaz için 2CDU ve Sığır Serum Albümini için 4JK4 gibi dört farklı antioksidan protein kullanılarak *in siliko* moleküler yerleştirme çalışmaları yapıldı. ADME ve toksisite (ADMEt) sonuçları, farmakokinetik, fiziko-kimyasal, ilaç benzerliği ve toksisite verilerinin tamamının potansiyel bir biyoaktif madde için uygun olduğunu gösterdi. Moleküler yerleştirme sonuçları, tüm yerleştirme sonuçlarının standarttan (Troloks) daha yüksek olduğunu göstermiştir. En iyi kenetlenme skoru (-9,4 kcal/mol), **3b** ligandı ile 2CDU proteini arasındaydı. Bileşiklerin TEAC değerleri de standarttan daha yüksekti ve bu da moleküler yerleştirme skorlarıyla uyumluydu. Elde edilen tüm verilerden, bileşik **3b**'nin potansiyel antioksidan özelliğe sahip olduğu sonucuna varılmıştır.

Novel Trifluoromethyl Containing Azo-Imin compounds: Synthesis, Characterization, and Investigation of Antioxidant Properties Using *In Vitro* and *In Silico* methods

Keywords
Schiff Base,
CUPRAC Method,
Antioxidant,
Molecular Docking,
ADMEt

Abstract: In this study, two new molecules 4-((4-methoxyphenyl)diazenyl)-2-(((4-(trifluoromethyl)phenyl)imino)methyl)phenol (**3a**) and 2-(((4-methoxyphenyl)imino)methyl)-4-((4-(trifluoromethyl)phenyl)diazenyl)phenol (**3b**) were synthesized. The ^{1}H-NMR, FTIR, UV-vis, and Mass analysis techniques were used to confirm the structures of the **3a** and **3b**. CUPRAC in vitro antioxidant activity method was also used to investigate the antioxidant properties of synthesized compounds. The compounds' ADME and toxicity parameters were also computed using SwissADME, Protox-II web servers respectively. I*n silico* Molecular docking studies were conducted utilizing four different antioxidant proteins, such as PDB ID: 1N8Q for Lipoxygenase, 1OG5 for CYP2C9, 2CDU for NADPH oxidase, and 4JK4 for Bovine Serum Albumin, to investigate the potential antioxidant properties of the synthesized compounds **3a** and **3b**. ADME and toxicity (ADMEt) results showed that pharmacokinetic, physico-chemical, drug-similarity, and toxicity data were all appropriate for a potential bioactive agent. Molecular docking results have shown that all docking results were higher than standard (Trolox). The best docking score (-9.4 kcal/mol) was between **3b** ligand and 2CDU protein. TEAC values of compounds were also higher than standard which was in harmony with molecular docking scores. From all obtained data It was concluded that the compound **3b** has the potential antioxidant agent.

** Corresponding author: tyesil@sinop.edu.tr*

1. Introduction

Free radical generation and antioxidant defense mechanisms are out of balance, which leads to the syndrome known as oxidative stress [1]. There are several potential causes of this imbalance, such as a lack of antioxidants in the diet, endogenous overproduction brought on by inflammation, or exposure to pro-oxidant elements in the environment [2]. In addition, many serious illnesses, including some metabolic disorders (diabetes, cancer), and neurodegenerative diseases, have oxidative stress as a key side effect [3,4]. Thus, it's necessary to develop novel antioxidants that can interact with free radicals or suppress their activity to stop oxidative damage. Primary and secondary antioxidants are two types of antioxidants. One of the primary classes of secondary metabolites present in plants is the source of phenolic chemicals. While metabolism is operating regularly, phenolic antioxidants can eliminate free radicals and stop reactive species from developing. Moreover, they can protect cells from lipid, protein, and nucleic acid damage, which can result in harm or death [5]. Because of this, they are often associated with delaying the beginning of some diseases, including diabetes, cancer, autoimmune disorders, neurological diseases, and cardiovascular diseases [6–8].

In organic chemistry, fluorine (F) is the smallest substituent that can be substituted with a hydrogen atom. In medicinal chemistry, the displacement of hydrogen atoms with F atoms is a common method. The main causes of this include fluorine's strong electron attraction, electrostatic interactions, small atomic size, and high lipophilicity. Research on the synthesis and biological functions of compounds containing fluorine, particularly those with the $-CF_3$ group, is growing continually [9,10]. Because of the significant influence that fluorine-containing compounds have on pharmaceutical growth, the US Food and Drug Administration (FDA) has approved over half of the most popular medicinal molecules [11].

Imines are substances with a double bond between carbon and nitrogen -C=N- and substituents at the carbon and nitrogen atoms that might be the same or different. When aldehydes combine with primary amines, commonly known as Schiff's base, an imine intermediate is created. It plays a crucial role not just in synthetic chemistry [12] but also in some biological activities such as antifungal [13], antibacterial [14], antimalarial [15], antiviral [16], anticancer [17], and antioxidant [18].

Azo compounds, which contain N=N- groups in structure, are among the most widely used chemical classes of organic compounds because of their wide range of applications in lasers, electro-optical devices, biomedical research, liquid crystal displays, textile dyeing, and inkjet printing and biological medical studies [19–21]. The synthesis of derivatives of azo compounds has generated considerable interest due to their wide biological activities and functions, which include antibacterial, anti-inflammatory, anthelminthic, antiviral, and anticancer effects [22]. The in silico and in vitro properties of synthesized azo compounds have been the subject of many studies of investigations in recent years [23]. After more research, the studies indicate that the produced azo compounds may have therapeutic potential [24–27].

Drug discovery is a difficult, costly, and time-consuming process that can take years and millions of dollars to complete. Therefore, recent technological and methodological advances have facilitated the development of computational methods, and it has been possible to quickly and easily discover new anticancer medications thanks to these developments. In developing and discovering new anti-cancer drugs, computational techniques such as computer-aided drug design, or CADD, have gained significance. Researchers can find compounds with the potential to be effective therapeutic candidates against a variety of diseases, by using computational methods (such as Absorption, Distribution, Metabolism, Elimination, Toxicity (ADMEt), Molecular Docking, etc). Furthermore, They can examine methodologies to simulate and predict the interactions between potential drug molecules and biological targets [28].

In the present study, new **3a** and **3b** compounds were synthesized and characterized via ^{1}H-NMR, FTIR, UV-Vis and Mass Spectrometer. The CUPRAC method was used to evaluate each molecule's *in vitro* antioxidant activity. The ADMEt parameters were predicted using the SwissADME ProTox-II and ADMETlab 2.0 server. Furthermore, the interaction of the synthesized compounds and some selected proteins (PDB ID: 1N8Q for Lipoxygenase, 1OG5 for CYP2C9, 2CDU for NADPH oxidase, and 4JK4 for Bovine Serum Albumin) associated with antioxidant properties was investigated using an *in silico* method. At the end of the molecular docking investigations, the ligand-protein interaction's quantities and properties were determined.

2. Material and Method

2.1. General information

All of the chemicals used for synthesis and purification were acquired from the companies Aldrich, Merck, and Isolab. Thin Layer Chromatography (TLC: SIL G/UV254 from MN GmbH & Co.) was utilized to monitor reaction conversion, and UV light (254 nm) was employed to see the spot. The Stuart SMP 30 was used to test the melting point of the synthesized compound in an open glass capillary tube. An Agilent 400 MHz spectrometer and DMSO-d_6 as a solvent were used to record NMR spectra. Parts per million (ppm) of chemical changes are shown for residual protons (DMSO-d_6: δ 2.50). FTIR spectrum was recorded using the Shimadzu IRSpirit

QATR-S, ν_{max} in cm^{-1}. A PG T80+ double beam spectrophotometer and a 1×10^{-4} M solution compound were utilized to record the UV-Vis spectrum. The Waters Radıan Asap Direct Mass Detector was employed for mass analyses. The full scan acquisition mode, ASAP+/ASAP ionization mode, gas (N_2), mass range of 100-1200 m/z, cone voltage of 10 V, isothermal heater temperature of 600 °C, corona current of 3 µA, and capillary dip sample technique were all incorporated in the analytical process.

2.2. Synthesis studies

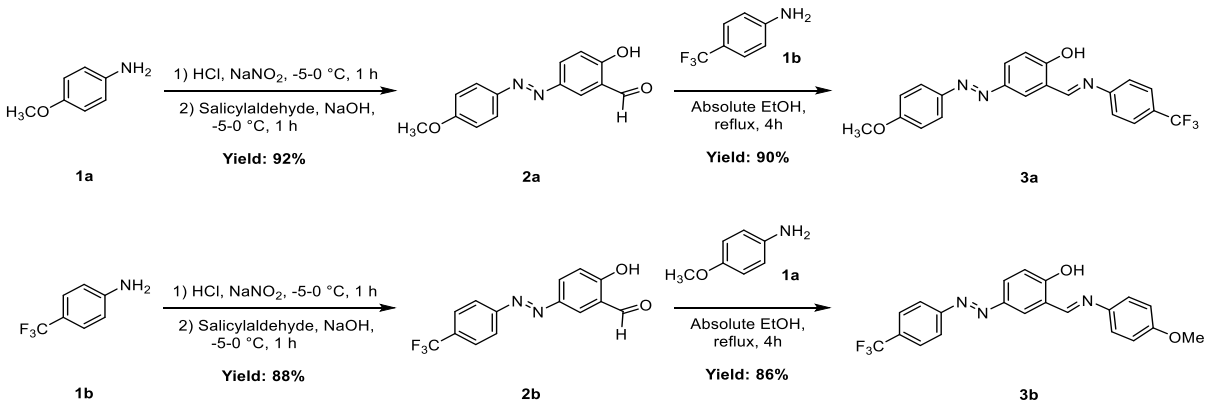

Figure 1. Synthesis Pathway for compounds **3a-b**

Synthesis of 2-hydroxy-5-((4-(methoxyphenyl)diazenyl)benzaldehyde (2a) compound: Synthesis Pathway for **2a** was shown in Figure 1. 4-methoxy aniline (10.0 mmol, 1.23 g) was dissolved in 2.1 mL of concentrated hydrochloric acid (25.0 mmol, 2.46 g) and 30 mL of distilled water in 50 mL beaker. After cooling the mixture to 0-(-5) ℃ using an ice-salt bath, $NaNO_2$ (10.0 mmol, 0.7 g) in 3 mL of distilled water was added dropwise while being continuously stirred. The diazonium salt formed after 1 h of stirring the mixture without allowing the temperature to increase above 0 ℃. In another beaker, the coupling reagent, Salicylaldehyde (10.0 mmol, 1.22 g) was dissolved in NaOH (20.0 mmol, 0.8 g in 10 mL of distilled water) solution, and the mixture was cooled to 0 ℃ with an ice-salt bath. After preparing the coupling mixtures, the diazonium salt solution was added dropwise and stirred for 1 h at 0-5 ℃. The resulting dark yellow precipitated solution was poured into beaker containing 100 mL of ice water and stirred for 1 h. After 1 h, the mixture was extracted with EtOAC (2 x 250 mL). The combined organic phases were dried with Na_2SO_4, filtered, and concentrated until approximately 20-25 mL of solvent remained by rotary evaporation in vacuo. The precipitated product was kept in the refrigerator (at 4 ℃) for overnight. The crude product was filtered, dried, and crystalized with EtOAc/Hexane (1:5, v/v). As the compound is known in the literature [29], only melting point and mass analyses were done to confirm the structure. **Yield:** 2.35 g, 92%. **Color:** Brown solid. **Mp:** 123–125 °C. **MS** = *m/z*: $[M+H]^+$ Calcd for $C_{14}H_{13}N_2O_3$, 257.09; Found: 257.24 (Figure 2).

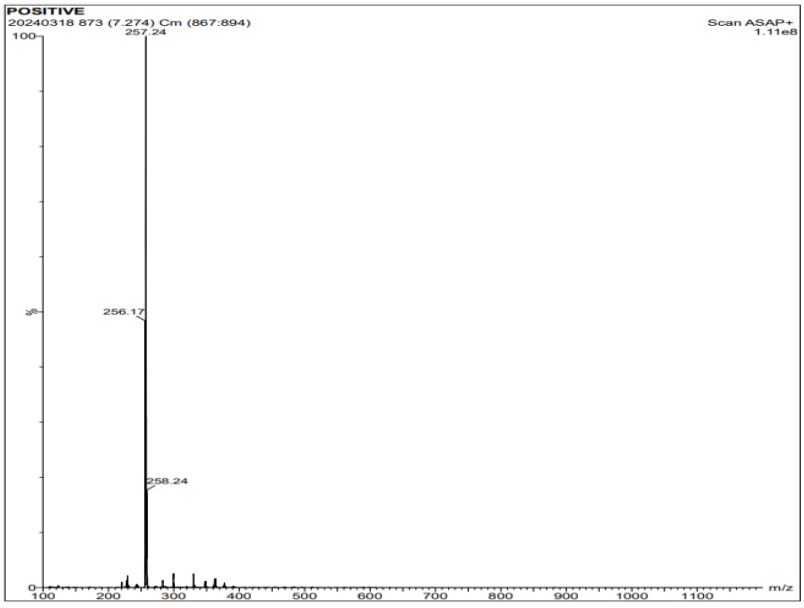

Figure 2. Mass spectrum of compound **2a**

Synthesis of 2-hydroxy-5-((4-(trifluoromethyl)phenyl)diazenyl)benzaldehyde (2b) compound: Synthesis Pathway for **2b** was shown in Figure 1. 4-trifluoromethylaniline (10.0 mmol, 1.61 g) was dissolved in 2.1 mL of concentrated hydrochloric acid (25.0 mmol, 2.46 g) and 30 mL of distilled water in 50 mL beaker. After cooling the mixture to 0-(-5) ℃ using an ice-salt bath, $NaNO_2$ (10.0 mmol, 0.7 g) in 3 mL of distilled water was added dropwise while being continuously stirred. The diazonium salt formed after 1 h of stirring the mixture without allowing the temperature to increase above 0 ℃. In another beaker, the coupling reagent, Salicylaldehyde (10.0 mmol, 1.22 g) was dissolved in NaOH (20.0 mmol, 0.8 g in 10 mL of distilled water) solution, and the mixture was cooled to 0 ℃ with an ice-salt bath. After preparing the coupling mixtures, the diazonium salt solution was added dropwise and stirred for 1 h at 0-5 ℃. The resulting dark yellow precipitated solution was poured into beaker containing 100 mL of ice water and stirred for 1 h. After 1 h, the mixture was extracted with EtOAC (2 x 250 mL). The combined organic phases were dried with Na_2SO_4, filtered, and concentrated until approximately 20-25 mL of solvent remained by rotary evaporation in vacuo. The precipitated product was kept in the refrigerator (at 4 ℃) for overnight. The crude product was filtered, dried, and crystalized with EtOAc/Hexane (1:5, v/v). As the compound is known in literature [30], only melting point and mass analyses were done to confirm the structure. **Yield:** 2.59 g, 88%. **Color:** Orange solid. **Mp:** 160–162 °C. **MS** = *m/z*: $[M+H]^+$ Calcd for $C_{14}H_{10}F_3N_2O_2$, 295.07; Found: 295.18 (Figure 3).

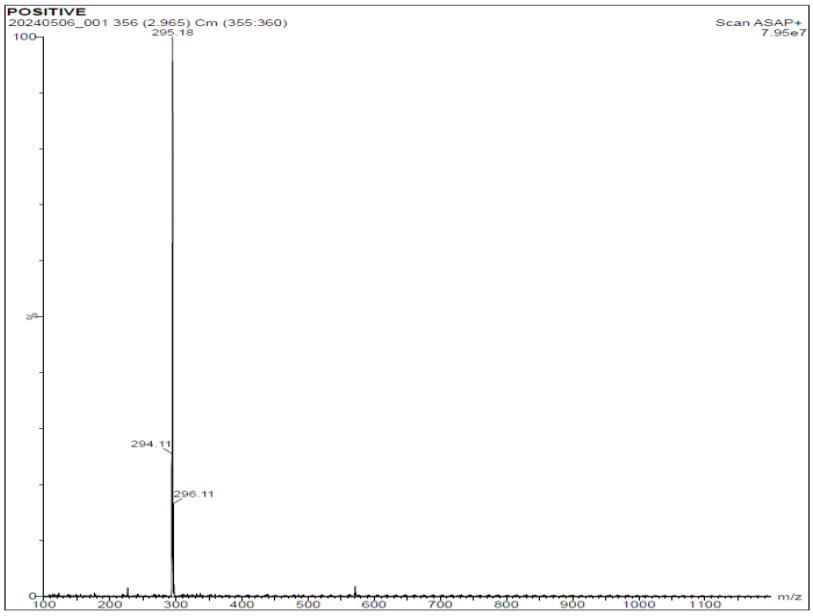

Figure 3. Mass spectrum of compound **2b**

Synthesis of 4-((4-methoxyphenyl)diazenyl)-2-(((4-(trifluoromethyl)phenyl)imino)methyl) phenol (3a) compound: Synthesis Pathway for **3a** was shown in Figure 1. A two-necked flask that had been oven-dried and equipped with a reflux condenser and magnetic stirring bar was charged with 1.1 mmol of 4-(trifluoromethyl)aniline (**1b**) and 25 mL of absolute ethanol. After clear solution was obtained, the 1 mmol 4-methoxy azoaldehyde (**2a**) was added to the flask. With the help of an oil bath, the flask was heated up until the solvent reflux point (approximately 85 °C). The conversion was followed by TLC and after the conversion was completed, half of the solvent was removed by rotary evaporation. After cooling the flask to room temperature, the precipitate was filtered and washed with n-hexane and cold ethanol. **Yield:** 90%. **Color:** Yellow solid. **Mp:** 195–197 °C. **FTIR (ATR):** $\tilde{\nu}_{max}$ (cm^{-1}) = 2946 (br, w), 2914 (w), 2840 (w), 1600 (s), 1485 (m), 1324 (s), 1276 (s), 1126 (s). **^{1}H NMR (400 MHz, DMSO-d_6)** δ 13.04 (s, 1H), 9.11 (s, 1H), 8.25 (s, 1H), 7.96 (d, J = 8.4 Hz, 1H), 7.90 – 7.78 (m, 4H), 7.60 (d, J = 7.7 Hz, 2H), 7.12 (dd, J = 12.9, 9.0 Hz, 3H), 3.84 (s, 3H) (Figure 4). **MS** = *m/z*: $[M+H]^+$ Calcd for $C_{21}H_{17}F_3N_3O_2$, 400.13; Found: 400.22 (Figure 5).

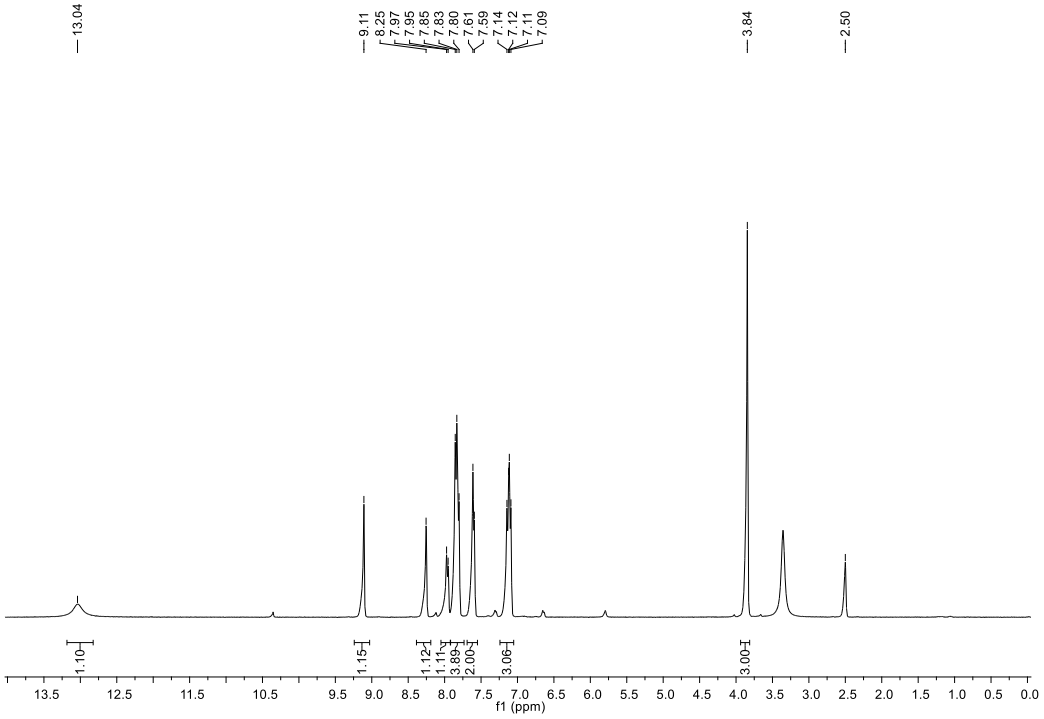

Figure 4. ^{1}H-NMR spectrometry of compound **3a**

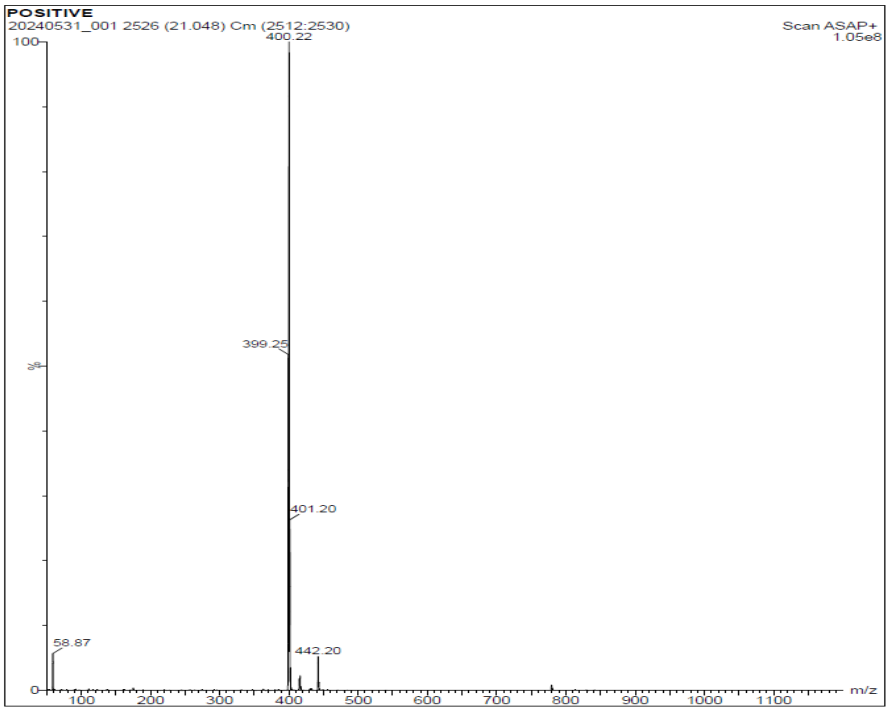

Figure 5. Mass spectrometry of compound **3a**

Synthesis of 2-(((4-methoxyphenyl)imino)methyl)-4-((4-(trifluoromethyl)phenyl)diazenyl)phenol (3b) compound: Synthesis Pathway for **3b** was shown in Figure 1. A two-necked flask that had been oven-dried and equipped with a reflux condenser and magnetic stirring bar was charged with 1.1 mmol of 4-methoxy aniline (**1a**) and 25 mL of absolute ethanol. After clear solution was obtained, the 1 mmol 4-trifluoro azoaldehyde (**2b**) was added to the flask. With the help of an oil bath, the flask was heated up until the solvent reflux point (approximately 85 °C). The conversion was followed by TLC and after the conversion was completed, half of the solvent was removed by rotary evaporation. After cooling the flask to room temperature, the precipitate was filtered and washed with n-hexane and cold ethanol. **Yield:** 86%. **Color:** Yellow solid. **Mp:** 186-188 °C. **FTIR (ATR):** $\tilde{\nu}_{max}$ (cm^{-1}) = 3024 (br, w), 2974 (w), 1620 (s), 1571 (m), 1508 (s), 1404 (s), 1350 (s), 1165 (s). **^{1}H NMR (400 MHz, DMSO-d_6)** δ 9.12 (s, 1H), 8.27 (d, J = 1.7 Hz, 1H), 7.95 (dd, *J* = 28.7, 8.5 Hz, 5H), 7.48 (d, *J* = 8.7 Hz, 2H), 7.12

(d, *J* = 8.9 Hz, 1H), 7.04 (d, *J* = 8.7 Hz, 2H), 3.80 (s, 3H) (Figure 6). **MS** = *m/z*: $[M+H]^+$ Calcd for $C_{21}H_{17}F_3N_3O_2$, 400.13; Found: 400.22 (Figure 7).

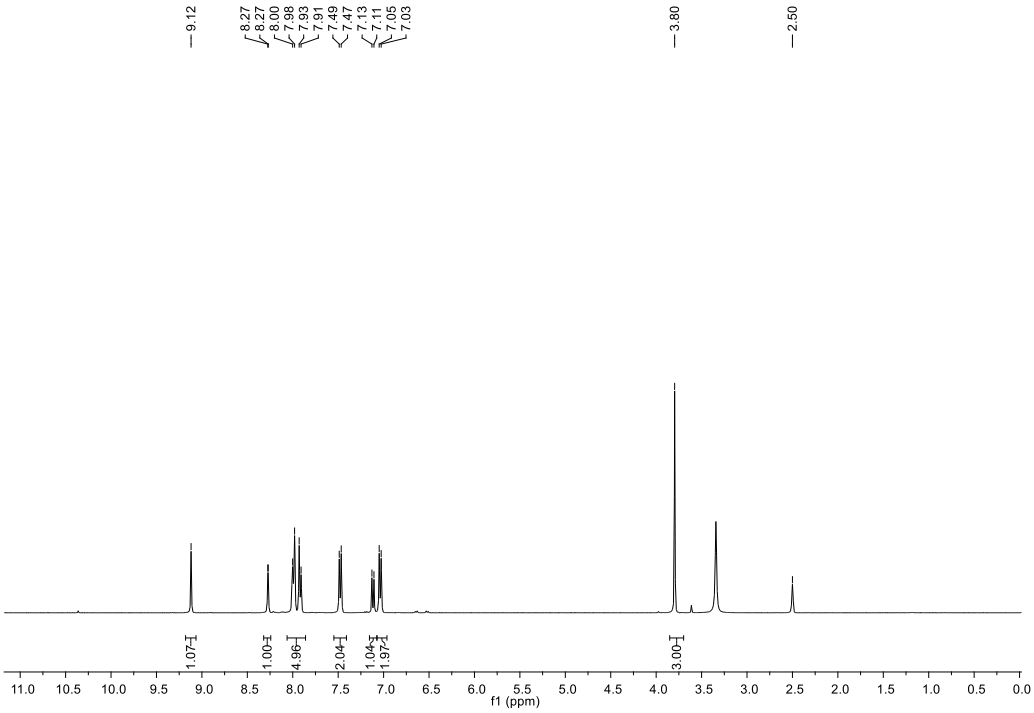

Figure 6. ^{1}H-NMR spectrometry of compound **3b**

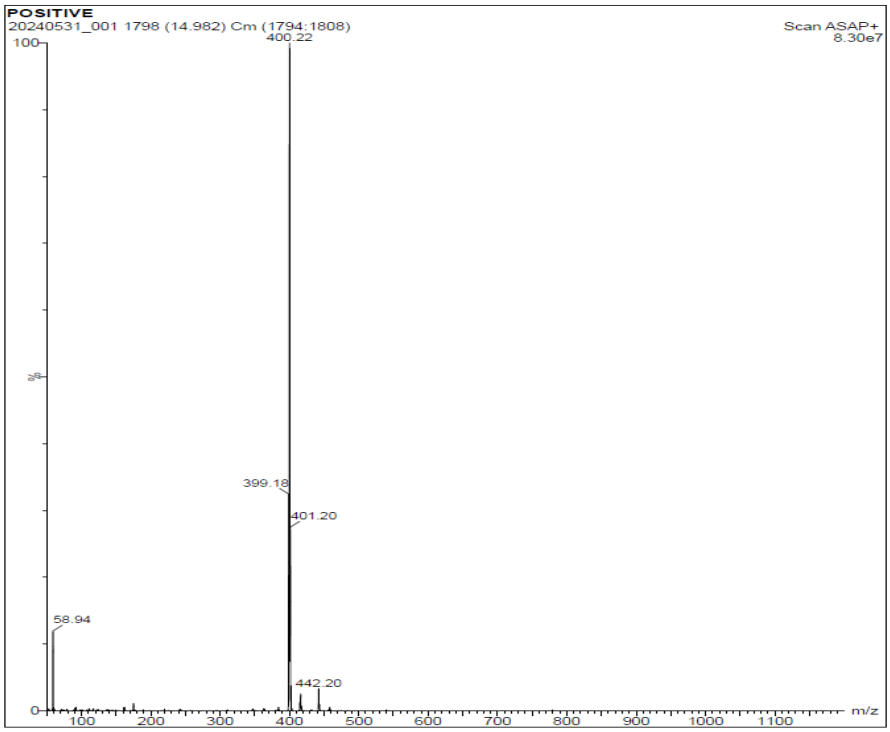

Figure 7. Mass spectrometry of compound **3b**

2.3. *In vitro* antioxidant activity studies

The antioxidant activities of synthesized compounds in absolute ethanol (**3a-b**) were determined using the CUPRAC method specified in literature. [31].

2.4. Computational studies

2.4.1. ADMEt properties

The ADME properties of **3a-b** compounds were calculated using the SwissADME web server [32].

Toxicity properties of **3a-b** compounds were determined via the Protox-II web server [33].

2.4.2. Geometry optimization

The structure of compounds **3a-b** was drawn in ChemBioDraw Ultra 14.0, Then the structures were transferred to ChemBio3D Ultra 14.0. The structures were saved as .mol2 files extension. .mol2 files were opened using Avogadro software [34]. The Structures were optimized using UFP parameters and optimized structures were saved as .mol2 file.

2.4.3. Molecular docking studies

The AutodockVina 1.1.2 [35] program was used for molecular docking investigations. All imaging processes were carried out using UCSF Chimera 1.17.3 for 3D [36] and BIOVIA Discovery Studio Visualizer for 2D [37]. For the molecular docking investigations, target proteins listed by PDB ID in Table 1 were utilized, and selected proteins (1N8Q, 1OG5, 2CDU, and 4JK4) were obtained as .pdb files from PDB Bank [38]. Using the UCSF Chimera 1.17.3 program, all heteroatoms, waters, and non-standard residues were eliminated from the protein. The proteins were prepared using UCSF Chimera 1.17.3 Dock Prep module. The 3D binding coordinates (*x,y,z*) of selected proteins were used as received in literature [39,40] and Molecular docking studies were conducted with proteins encircled by a grid box (40 x 40 x 40 $Å^3$).

Table 1. Selected proteins with PDB ID and binding coordinates for Molecular Docking studies

Proteins and PDB IDs		Coordinates and Values		
Protein	**PDB ID**	**X**	**Y**	**Z**
Lipoxygenase	1N8Q	22.45	1.29	20.36
CYP2C9	1OG5	-19.82	86.68	38.27
NADPH Oxidase	2CDU	18.99	-5.77	-1.80
Bovine Serum Albumin (BSA)	4JK4	95.87	16.04	13.49

3. Results

3.1. UV-Vis absorbance measurements

UV absorbance measurements were performed using a 1 × 10^{-4} M solution of the synthesized compound in DMSO between 200 and 900 nm to identify the maximum wavelengths of compounds **3a-b**. Table 2 provides the maximum wavelengths of compounds **3a–b**, and Figure 8 shows the UV–Vis spectra.

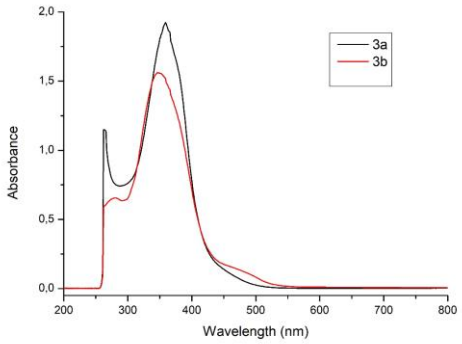

Figure 8. UV-Vis spectras of compound **3a-b**

The maximum absorbance values of the synthesized compounds were significant because absorbance measurements of antioxidant activity investigations were carried out at 450 nm. There was no maximum found at 450 nm when the maximum absorbance values were assessed. When the maximum wavelengths of the synthesized compounds were examined, it was observed that both of them had two maximum wavelengths. The first maximum wavelengths of the compounds were determined as 263 nm for **3a**, 281 nm for **3b**, and the second maximum wavelengths were determined as 359 nm and 346 nm, respectively.

Table 2. The maximum wavelengths of compounds **3a–b**

Compound	Maximum Wavelengths
3a	359, 263
3b	346, 281

3.2. *In vitro* antioxidant activity studies

The CUPRAC technique has been extensively studied in the literature for determining the antioxidant properties of synthesized compounds. TEAC (Trolox Equivalents antioxidant Capacity) value has important to do meaningful comparison of synthesized compounds against the trolox standard. 1.0 x 10^{-3} M stock solution containing all synthesized compounds (**3a–b**) was prepared in absolute ethanol. Five distinct solutions containing different concentrations of synthesized compounds were prepared using 1 x 10^{-3} M, and the CUPRAC method was used to investigate their antioxidant properties. To create calibration curves, the investigations were conducted three times, and mean data were obtained. Table 3 displayed the TEAC values of synthesized compounds and trolox.

Table 3. TEAC values of compounds (**3a-b**) and Trolox at 450 nm

	Compound 3a	Compound 3b	Trolox
TEAC	1.09	1.13	1.0

Antioxidant activity and TEAC levels are directly correlated. When the TEAC values of the synthesized

compounds (**3a-b**) are examined (Table 3), it can be said that they are higher than Trolox (TEAC > 1) and therefore have higher antioxidant activity than Trolox.

3.3. Computational studies

3.3.1. ADMEt properties

A crucial initial phase in the development of any pharmaceutical compound is determining the ADMEt parameters of a new drug candidate. Most candidate compounds are eliminated for a variety of reasons, including their incorrect pharmacokinetics and drug-likeness [41]. ADMEt properties of compounds (**3a-b**) were demonstrated in Table 4.

According to Lipinski's rules, the drug candidate should have a molecular weight of between 150 and 500 g/mol, an MLOGP value of less than 4.15, fewer than 10 hydrogen bond acceptor atoms, and fewer than 5 hydrogen bond donor atoms. When the physicochemical parameters of the synthesized molecules **3a** and **3b** were assessed, it was found that their molecular weights were 399.37 g/mol. Compounds **3a** and **3b** were accepted by Lipinski after being examined for molecular weight and all other criteria. Compounds' ability to penetrate cell membranes is determined by their TPSA value, which is also important and should be less than 140 Å[42]. The TPSA values of compounds **3a** and **3b** were calculated 66.54 $Å^2$.

The term "lipophilicity" describes a lipid's ability to dissolve in water. Drug molecules must pass through a number of biological barriers, including as the skin, the gut, and the blood-brain barrier, in order to reach their target locations. Therefore, a molecule must break down at specific rates in both oil and water. When Table 4 was examined, the lipophilicity (CLog$P_{o/w}$) number of compounds **3a** and **3b** were calculated 5.43 and 5.37, respectively.

BOILED-Egg graphs were used to calculate the ADME parameters, the blood-brain barrier, and gastrointestinal absorption (GI). In this diagram, the yellow area denotes possible BBB permeability locations, whereas the white area shows possible GI absorption sites. P-gp is shown as an active substrate by blue spots (PGP+) and as an inactive substrate by red dots (PGP-)[32]. When Figure 9 was examined, The presence of compounds **3a** and **3b** in the outer gray zone indicated that they had limited brain permeability and low absorption.

Compounds **3a** and **3b** were found to have toxicity properties that could be determined using the widely used Protox-II web server. Upon analyzing Table 4, The LD50 (Lethal Dose) value of each compound was determined to be 1500 mg/kg. Protox-II web server was also used to evaluate the toxicity class of compounds. When the toxicity level was compared from 1st (the worst) to 6th (the best), compounds **3a** and **3b** were found to be in the fourth class.

Table 4. ADME and Toxicity Properties of compounds **3a-b**

Compounds		**3a**	**3b**
Lipinski's Rule of Five	Molecular Weight (g/mol) ≤ 500	399.37	399.37
	MLogP ≤ 4.15	3.89	3.62
	Hydrogen Bond Acceptor ≤ 10	8	8
	Hydrogen Bond Donor ≤ 5	1	1
	Lipinski	Yes	Yes
Physicochemical Properties	TPSA ($Å^2$)	66.54	66.54
Lipophilicity Properties	Consensus Log $P_{o/w}$	5.43	5.37
	WLogP	7.74	7.74
Pharmacokinetic Properties	GI	Low	Low
Toxicity Properties	LD50 (mg/kg)	1500	1500
	Toxicity Class	4	4

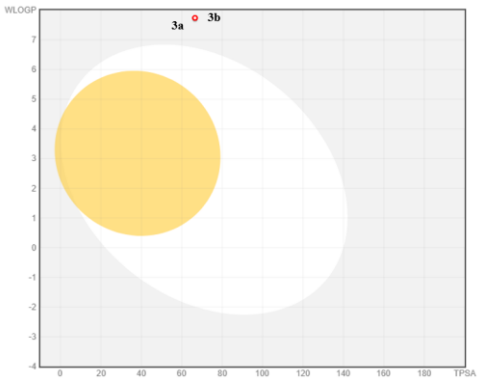

Figure 9. Boiled-Egg diagram of compounds **3a-b**

3.3.2. Molecular docking studies

Molecular docking, an effective method based on receptor-ligand interactions, involves docking small molecules into the receptor's binding site to estimate the complex's binding affinity [43]. AutodockVina 1.1.2 was used to conduct molecular docking investigations of all synthesized compounds. For molecular docking studies of compounds and standard antioxidant Trolox were performed on proteins associated with antioxidants that had encoded by PDB IDs of 1N8Q, 1OG5, 2CDU, and 4JK4. All synthesized molecule was individually docked to distinct protein coordinates, encircling the active region of the protein with a 40 x 40 x 40 $Å^3$ grid box. The Docking scores of compounds (**3a-b**), which ranged from -8.3 kcal/mol to -9.4 kcal/mol, were depicted in Table 5. The protein-ligand complex pairing 1N8Q-**3b**, 1OG5-**3a**, 2CDU-**3b**, and 4JK4-**3b** had the highest docking scores. The 2CDU-**3b** complex has the best docking scores (ΔG: -9.4 kcal/mol) than Trolox and among all ligand complexes. It was observed that these data were compatible with in vitro antioxidant results. Table 6 analysis shows that hydrogen bonds, carbon-hydrogen bonds, halogen, π-cation, alkyl, and π-alkyl bonds are the interactions between 2CDU and **3b** complexes. There are two hydrogen bonds between 2CDU-**3b** complex. These bonds have a length of 2.09 Å between ASP179 aminoacid and phenolic -OH group, 2.28 Å between WAL214 aminoacid and methoxy oxygen group.

Table 5. Docking scores of compounds **3a-b** and Trolox

PDB ID	Compounds		Standard
	3a	3b	Trolox
1N8Q	-8.3	-8.5	-6.9
1OG5	-8.6	-8.5	-7.2
2CDU	-9.2	-9.4	-7.2
4JK4	-8.5	-8.8	-6.7

Table 6. 2D and 3D representation of 2CDU-**3b** interaction

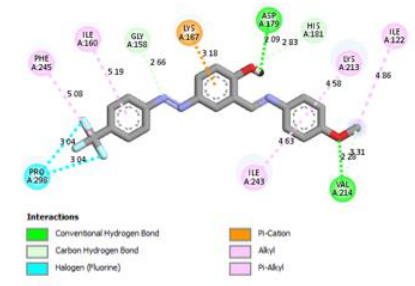	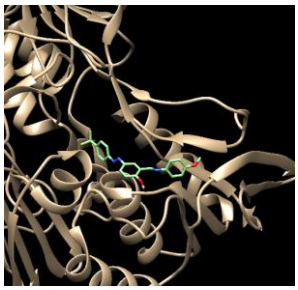	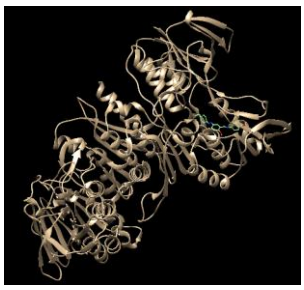
2CDU-3b		

Discussion and Conclusion

In this study, Novel Trifluoromethyl Containing Azo-Imincompounds (**3a-b**) were synthesized (*Yield*: 90-86 %) and were characterized by using The ^{1}H-NMR, FT-IR, UV-vis, and Mass analysis techniques to confirm the structures of compounds. SwissADME and Protox-II web services were utilized to calculate the toxicity and ADME parameters of the compounds, respectively. According to ADME and toxicity (ADMEt) results, the drug-similarity, pharmacokinetic, physico-chemical, and toxicity data were all within acceptable level for a potential bioactive agent. To investigate the potential antioxidant properties of the synthesized compounds **3a** and **3b**, molecular docking studies were carried out using four distinct antioxidant proteins, such as PDB ID: 1N8Q for lipoxygenase, 1OG5 for CYP2C9, 2CDU for NADPH oxidase, and 4JK4 for bovine serum albumin. All of the docking results from molecular docking were higher than trolox. The interaction between the 2CDU protein and the **3b** ligand had the best docking score (-9.4 kcal/mol). The antioxidant properties of the compound **3a** and **3b** were also examined using the CUPRAC in vitro antioxidant activity method. When the TEAC values of the compounds were examined, the TEAC value was above the trolox values and this was compatible with the molecular docking scores. Based on all of the data obtained, it was determined that compound **3b** can potential antioxidant agent.

Declaration of Ethical Code

In this study, we undertake that all the rules required to be followed within the scope of the "Higher Education Institutions Scientific Research and Publication Ethics Directive" are complied with and that none of the actions stated under the heading "Actions Against Scientific Research and Publication Ethics" are not carried out.

References

[1] Sies, T. 2020. Oxidative Stress: Concept and Some Practical Aspects. Antioxidants, 9, 852.

[2] Preiser, J. 2012. Oxidative Stress. Journal of Parenteral and Enteral Nutrition, 36, 147–154.

[3] Matés, J. M., Segura, J. A., Alonso, F. J., Márquez, J. 2012. Oxidative stress in apoptosis and cancer: an update. Archives of Toxicology, 86, 1649–1665.

[4] Houldsworth, A. 2023. Role of oxidative stress in neurodegenerative disorders: a review of reactive oxygen species and prevention by antioxidants. Brain Communications, 6.

[5] Zhang, Y., Seeram, N. P., Lee, R., Feng, L., Heber, D. 2008. Isolation and Identification of Strawberry Phenolics with Antioxidant and Human Cancer Cell Antiproliferative Properties, Journal of Agricultural and Food Chemistry, 56, 670–675.

[6] Kaur, S., Das, M. 2011. Functional foods: An overview. Food Science and Biotechnology, 20, 861–875.

[7] Alarcón-Flores, M. I., Romero-González, R., Vidal, J. L. M., Frenich, A. G. 2013. Multiclass determination of phytochemicals in vegetables and fruits by ultra-high-performance liquid chromatography coupled to tandem mass spectrometry. Food Chemistry, 141, 1120–1129.

[8] Pallauf, K., Bendall, J. K., Scheiermann, C., Watschinger, K., Hoffmann, J., Roeder, T., Rimbach, G. 2013. Vitamin C and lifespan in model organisms. Food and Chemical Toxicology, 58, 255–263.

[9] Abula, A., Xu, Z., Zhu, Z., Peng, C., Chen, Z., Zhu, W., Aisa, H. A. 2020. Substitution Effect of the Trifluoromethyl Group on the Bioactivity in Medicinal Chemistry: Statistical Analysis and Energy Calculations. Journal of Chemical Information and Modeling, 60, 6242–6250.

[10] Sap, J. B. I., Straathof, N. J. W., Knauber, T., Meyer, C.F., Médebielle, M., Buglioni, L., Genicot, C., Trabanco, A. A., Noël, T., am Ende, C. W., Gouverneur, V. 2020. Organophotoredox Hydrodefluorination of Trifluoromethylarenes with Translational Applicability to Drug Discovery. Journal of the American Chemical Society, 142, 9181–9187.

[11] Swallow, S. 2015. Fluorine in Medicinal Chemistry. pp. 65–133. Lawton, G., Witty, D. R., ed. Progress in Medicinal Chemistry, Elsevier B.V.

[12] Dilek, Ö., Dede, B., Karabacak Atay, Ç., Tilki, T. 2024. Promising agent for the efficient extraction of Co(II) ions from aqueous medium and its metal complexes: Synthesis, theoretical calculations and solvent extraction. Polyhedron, 250, 116843.

[13] Wei, L., Tan, W., Wang, G., Li, Q., Dong, F., Guo, Z. 2019. The antioxidant and antifungal activity of chitosan derivatives bearing Schiff bases and quaternary ammonium salts. Carbohydrate Polymers, 226, 115256.

[14] Haj Mohammad Ebrahim Tehrani, K., Hashemi, M., Hassan, M., Kobarfard, F., Mohebbi, S. 2016. Synthesis and antibacterial activity of Schiff bases of 5-substituted isatins. Chinese Chemical Letters, 27, 221–225.

[15] Bekhit, A. A., Saudi, M. N., Hassan, A. M. M., Fahmy, S. M., Ibrahim, T. M., Ghareeb, D., El-Seidy, A. M., Nasralla, S. N., Bekhit, A.E.-D.A. 2019. Synthesis, in silico experiments and biological evaluation of 1,3,4-trisubstituted pyrazole derivatives as antimalarial agents. European Journal of Medicinal Chemistry, 163, 353–366.

[16] Iacopetta, D., Ceramella, J., Catalano, A., Saturnino, C., Bonomo, M. G., Franchini, C., Sinicropi, M. S. 2021. Schiff Bases: Interesting Scaffolds with Promising Antitumoral Properties. Applied Sciences, 11, 1877.

[17] Dilek, Ö. 2024. Imidazole Based Novel Schiff Base: Synthesis, Characterization, Quantum Chemical Calculations, In Silico Investigation of ADMEt Properties and Molecular Docking Simulations against VEGFR2 Protein. Bitlis Eren Üniversitesi Fen Bilimleri Dergisi, 13, 62–78.

[18] Kitouni, S., Chafai, N., Chafaa, S., Houas, N., Ghedjati, S., Djenane, M. 2023. Antioxidant activity of new synthesized imine and its corresponding α-aminophosphonic acid: Experimental and theoretical evaluation. Journal of Molecular Structure, 1281, 135083.

[19] Huang, D. D., Pozhidaev, E. P., Chigrinov, V. G., Cheung, H. L., Ho, Y. L., Kwok, H. S. 2004. Photo-aligned ferroelectric liquid crystal displays based on azo-dye layers. Displays, 25, 21–29.

[20] Borbone, F., Carella, A., Ricciotti, L., Tuzi, A., Roviello, A., Barsella, A. 2011. High nonlinear optical response in 4-chlorothiazole-based azo dyes. Dyes and Pigments, 88, 290–295.

[21] El-Sonbati, A. Z., Diab, M. A., El-Bindary, A. A., Shoair, A. F., Hussein, M. A., El-Boz, R. A. 2017. Spectroscopic, thermal, catalytic and biological studies of Cu(II) azo dye complexes. Journal of Molecular Structure, 1141, 186–203.

[22] Mitra, A., Mawson, A. 2017. Neglected Tropical Diseases: Epidemiology and Global Burden.

Tropical Medicine and Infectious Disease, 2, 36.

[23] Karabacak Atay, Ç., Dilek, Ö., Tilki, T., Dede, B. 2023. A novel imidazole-based azo molecule: synthesis, characterization, quantum chemical calculations, molecular docking, molecular dynamics simulations and ADMET properties. Journal of Molecular Modeling, 29, 226.

[24] Saeed, A. M., AlNeyadi, S. S., Abdou, I. M. 2020. Anticancer activity of novel Schiff bases and azo dyes derived from 3-amino-4-hydroxy-2H-pyrano[3,2-c]quinoline-2,5(6H)-dione. Heterocyclic Communications, 26, 192–205.

[25] Chhetri, A., Chettri, S., Rai, P., Mishra, D. K., Sinha, B., Brahman, D. 2021. Synthesis, characterization and computational study on potential inhibitory action of novel azo imidazole derivatives against COVID-19 main protease (Mpro: 6LU7). Journal of Molecular Structure, 1225.

[26] Kasare, M. S., Dhavan, P. P., Shaikh, A. H. I., Jadhav, B. L., Pawar, S.D. 2022. Novel Schiff base scaffolds derived from 4-aminoantipyrine and 2-hydroxy-3-methoxy-5-(phenyldiazenyl) benzaldehyde: Synthesis, antibacterial, antioxidant and anti-inflammatory. Journal of Molecular Recognition, 35.

[27] Maliyappa, M. R., Keshavayya, J., Sudhanva, M.S., Pushpavathi, I., Kumar, V. 2022. Heterocyclic azo dyes derived from 2-(6-chloro-1,3-benzothiazol-2-yl)-5-methyl-2,4-dihydro-3H-pyrazol-3-one having benzothiazole skeleton: Synthesis, structural, computational and biological studies. Journal of Molecular Structure, 1247, 131321.

[28] Niu, Y., Lin, P. 2023. Advances of computer-aided drug design (CADD) in the development of anti-Azheimer's-disease drugs. Drug Discovery Today, 28, 103665.

[29] Khanmohammadi, H., Khodam, F. 2013. Solvatochromic and electrochemical properties of new thermally stable azo–azomethine dyes with $N_2S_2O_2$ donor set of atoms. Journal of Molecular Liquids, 177, 198–203.

[30] Sun, Y. F., Xu, S. H., Wu, R. T., Wang, Z. Y., Zheng, Z. B., Li, J. K., Cui, Y. P. 2010. The synthesis, structure and photoluminescence of coumarin-based chromophores. Dyes and Pigments, 87(2), 109-118.

[31] Apak, R., Güçlü, K., Özyürek, M., Çelik, S.E. 2008. Mechanism of antioxidant capacity assays and the CUPRAC (cupric ion reducing antioxidant capacity) assay. Microchimica Acta, 160, 413–419.

[32] Daina, A., Michielin, O., Zoete, V. 2017. SwissADME: a free web tool to evaluate pharmacokinetics, drug-likeness and medicinal chemistry friendliness of small molecules. Scientific Reports, 7, 42717.

[33] Banerjee, P., Eckert, A. O., Schrey, A. K., Preissner, R. 2018. ProTox-II: a webserver for the prediction of toxicity of chemicals. Nucleic Acids Research, 46, 257–263.

[34] Hanwell, M. D., Curtis, D. E., Lonie, D. C., Vandermeersch, T., Zurek, E., Hutchison, G. R. 2012. Avogadro: an advanced semantic chemical editor, visualization, and analysis platform. Journal of Cheminformatics, 4, 17.

[35] Trott, O., Olson, A. J. 2010. AutoDock Vina: Improving the speed and accuracy of docking with a new scoring function, efficient optimization, and multithreading. Journal of Computational Chemistry, 31, 455–461.

[36] Pettersen, E. F., Goddard, T. D., Huang, C. C., Couch, G. S., Greenblatt, D. M., Meng, E. C., Ferrin, T. E. 2004. UCSF Chimera-A visualization system for exploratory research and analysis. Journal of Computational Chemistry, 25, 1605–1612.

[37] BIOVIA (2021). Discovery Studio Visualizer, version 21.1.0.20298. Dassault Systèmes, San Diego, CA.

[38] Berman, H. M. 2000. The Protein Data Bank. Nucleic Acids Research, 28, 235–242.

[39] Kandsi, F., Elbouzidi, A., Lafdil, F. Z., Meskali, N., Azghar, A., Addi, M., Hano, C., Maleb, A., Gseyra, N. 2022. Antibacterial and Antioxidant Activity of Dysphania ambrosioides (L.) Mosyakin and Clemants Essential Oils: Experimental and Computational Approaches. Antibiotics, 11, 482.

[40] Bouzammit, R., Lakkab, I., El fadili, M., Kanzouai, Y., Chalkha, M., Nakkabi, A., El Bali, B., Obbade, S., Jouffret, L., Lachkar, M., Al Houari, G. 2024. Synthesis, crystal structure, antioxidant activity and molecular docking studies of 2-(1-(3-methyl-1-oxo-1,2,3,4-tetrahydronaphthalen-2-yl)ethyl)malononitrile. Journal of Molecular Structure, 1312, 138582.

[41] Ulutürk, M., Karabacak Atay, Ç., Dede, B., Tilki, T. 2023. Potentially Bioactive Novel Isophthalic Acid Based Azo Molecules: Synthesis, Characterization, Quantum Chemical Calculations, ADMET Properties, Molecular Docking and Molecular Dynamics Simulations. Polycyclic Aromatic Compounds, 1–22.

[42] Veber, D. F., Johnson, S. R., Cheng, H. Y., Smith, B. R., Ward, K. W., Kopple, K. D. 2002. Molecular Properties That Influence the Oral

Bioavailability of Drug Candidates. Journal of Medicinal Chemistry, 45, 2615–2623.

[43] Lakhera, S., Devlal, K., Ghosh, A., Rana, M. 2021. In silico investigation of phytoconstituents of medicinal herb 'Piper Longum' against SARS-CoV-2 by molecular docking and molecular dynamics analysis. Results in Chemistry, 3, 100199.